INTERNATIONAL JOURNAL FOR NUMERICAL AND ANALYTICAL METHODS IN GEOMECHANICS
Int. J. Numer. Anal. Meth. Geomech., **24,** 101–133 (2000)

ON THE VOLUMETRIC DEFORMATION OF RECONSTITUTED SOILS

M. D. LIU AND J. P. CARTER*

Department of Civil Enginering, The University of Sydney, N.S.W. 2006, Australia

SUMMARY

This paper reviews the phenomenon of volumetric hardening, which is a common feature of the mechanical behaviour of many geo-materials. Three different material idealizations have been proposed to describe this hardening, and the paper contains the corresponding mathematical formulation. These idealizations vary in their complexity and hence their ability to capture different aspects of real material behaviour. Any of the three postulates can be implemented into most constitutive models. As a demonstration of their capabilities, the postulates have been implemented into the well-known modified Cam Clay model, and computations are made with the resulting new constitutive models. It is seen that the new models can successfully represent important features of soil behaviour such as plastic yielding associated with loading inside the current virgin yield surface, the loosening or densifying of granular soils caused by shearing, and the accumulation of both volumetric and distortional deformation caused by repeated drained loading over a large number of cycles.

KEY WORDS: reconstituted soil; volumetric hardening; material idealization; constitutive equations

1. INTRODUCTION

It is common practice in soil mechanics to adopt the voids ratio as a state parameter. The volumetric strain experienced by an element of soil can be related conveniently to changes in voids ratio and the initial voids ratio, i.e. its initial state. Many soils and other materials exhibit volumetric hardening when subjected to both isotropic and deviatoric stress changes, and so it would seem obvious to use the voids ratio as a measure of the hardening that occurs. Various stress–strain models developed using this approach are available in the literature.[1–5]

This paper is concerned with the manner in which the concept of plastic volumetric hardening may be incorporated into constitutive models of particulate materials, including those used to describe the mechanical behaviour of reconstituted soils. Three idealizations (referred here as 'postulates') are described. The corresponding mathematical formulae describing the hardening are also presented, with each employing implicitly the plastic volumetric deformation as a state parameter. The proposed material idealizations are quite general and symbolize the relationship between the current stress state, voids ratio and the stress history. Each postulate can be used to develop a new constitutive model, or can be implemented into many existing soil models.

* Correspondence to: Professor John P. Carter, Department of Civil Engineering, University of Sydney, NSW 2006, Australia. E-mail: J.Carter@civil.usyd.edu.au

Contract/grant sponsor: Australian Research Council

CCC 0363–9061/2000/020101–33$17.50

Received 30 March 1998
Revised 16 April 1999

To demonstrate the detailed procedures required for implementation, the three postulates are separately implemented into the well-known modified Cam Clay soil model. The new constitutive models resulting from these implementations are then used to predict the behaviour of soil under various loadings, including monotonic and cyclic shear loading. The postulates are then evaluated in light of the model performance.

Attention is restricted here to the case of reconstituted soils, and so the influence of soil structure has been specifically ignored. It is planned to address the issue of soil structure in a future paper. For clarity and convenience, attention is also confined to loading cases that involve fully drained soil behaviour. Predictions of the volumetric and deviatoric strains that develop under various loadings have been made. However, the models developed in this paper could also be used in calculations of undrained behaviour of soils, where volumetric strains is prohibited and the key response parameter becomes the excess pore water pressure.

2. DESCRIPTIONS OF STRESS AND STRAIN

Before proceeding to the formulation of constitutive equations, it is necessary to define various quantities for stress and strain. It will be assumed that the current state of the soil can be described by its voids ratio, denoted by e, and the following stress quantities.

The mean stress is given by

$$p' = \tfrac{1}{3}(\sigma'_{11} + \sigma'_{22} + \sigma'_{33}) \tag{1}$$

and the generalized deviatoric stress by

$$q = \frac{1}{\sqrt{2}} \sqrt{[(\sigma'_{11} - \sigma'_{22})^2 + (\sigma'_{22} - \sigma'_{33})^2 + (\sigma'_{33} - \sigma'_{11})^2 + 6(\sigma'^2_{12} + \sigma'^2_{23} + \sigma'^2_{31})]} \tag{2}$$

in which σ'_{ij} are the Cartesian components of effective stress.

The corresponding volumetric and deviatoric strains are

$$\varepsilon_v = \varepsilon_{11} + \varepsilon_{22} + \varepsilon_{33} \tag{3}$$

and

$$\varepsilon_d = \frac{\sqrt{2}}{3} \sqrt{[(\varepsilon_{11} - \varepsilon_{22})^2 + (\varepsilon_{22} - \varepsilon_{33})^2 + (\varepsilon_{33} - \varepsilon_{11})^2 + 6(\varepsilon^2_{12} + \varepsilon^2_{23} + \varepsilon^2_{31})]} \tag{4}$$

3. THREE POSTULATES ON VOLUMETRIC DEFORMATION

The fundamental assumption of this work is that the hardening of soil is governed by plastic volumetric strain. A consequence of this assumption is that all stress states which have the same accumulation of plastic volumetric strain constitute a single yield surface. Because the elastic volumetric deformation can be calculated from the current stress state, the value of the voids ratio minus the elastic contribution thus uniquely defines the plastic volumetric strain. Therefore, the size of the yield surface is related to the current voids ratio, and the current stress state from which the elastic volumetric deformation is computed. The size of the yield surface is denoted by p'_0, the intercept of the yield surface on the isotropic (or p' axis) in stress space (see Figure 2).

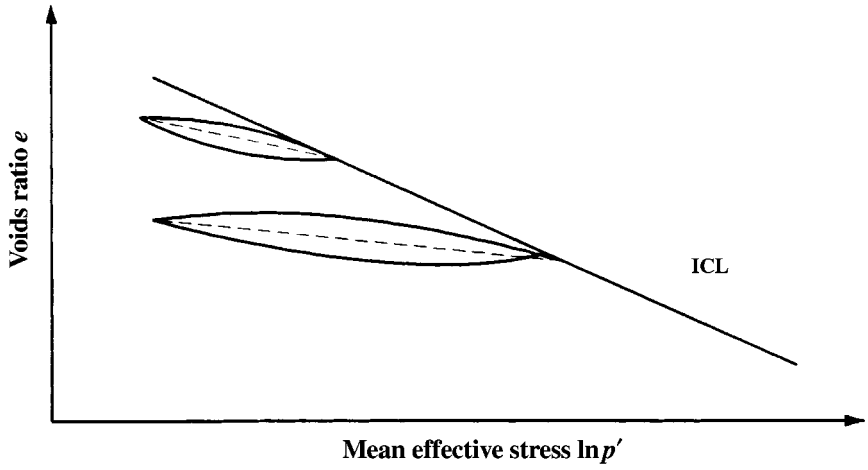

Figure 1. Soil behaviour under isotropic loading

An isotropic loading test on an initially normally consolidated soil typically produces a relationship between voids ratio, e, and mean effective stress, p', as shown schematically in Figure 1. The mean stress has been plotted on a logarithmic scale, and to a first approximation a linear relationship is often assumed for virgin yielding, with a gradient of λ. However, during cyclic loading a Bauschinger effect is commonly observed. The slope of the best fit straight line through the unloading–reloading loop is designated as κ.

In the following sections, three different material idealizations are proposed. As these idealizations are consecutively introduced, the level of model complexity is increased to capture additional features of soil behaviour. In this first, no attempt is made to allow for the Bauschinger effect, and so this simplest description of hardening is unlikely to be effective in situations that involve repeated stress reversal. Hysteresis is dealt within the second idealization, while in the third, an idealization that allows economical prediction of the response of soil subjected to many repeated applications of loading is introduced. It should also be noticed that the proposed Postulates describe only the plastic volumetric deformation associated with various loading. The elastic deformation and the corresponding plastic distortional deformation are to be decided according to the particular model into which a postulate is implemented. The corresponding plastic distortional deformation is usually computed from the plastic volumetric deformation via the flow rule.

3.1. Material idealization I: Elasticity and virgin-yielding

It is natural to begin with the simplest description of the hardening of soil. This idealization is well known, but is included here for completeness. It can be expressed in the form of a postulate.

Postulate I. Soil is idealized as an elastic and virgin-yielding material. The yield surface varies isotropically with the change in plastic volumetric deformation. Soil behaviour inside the yield

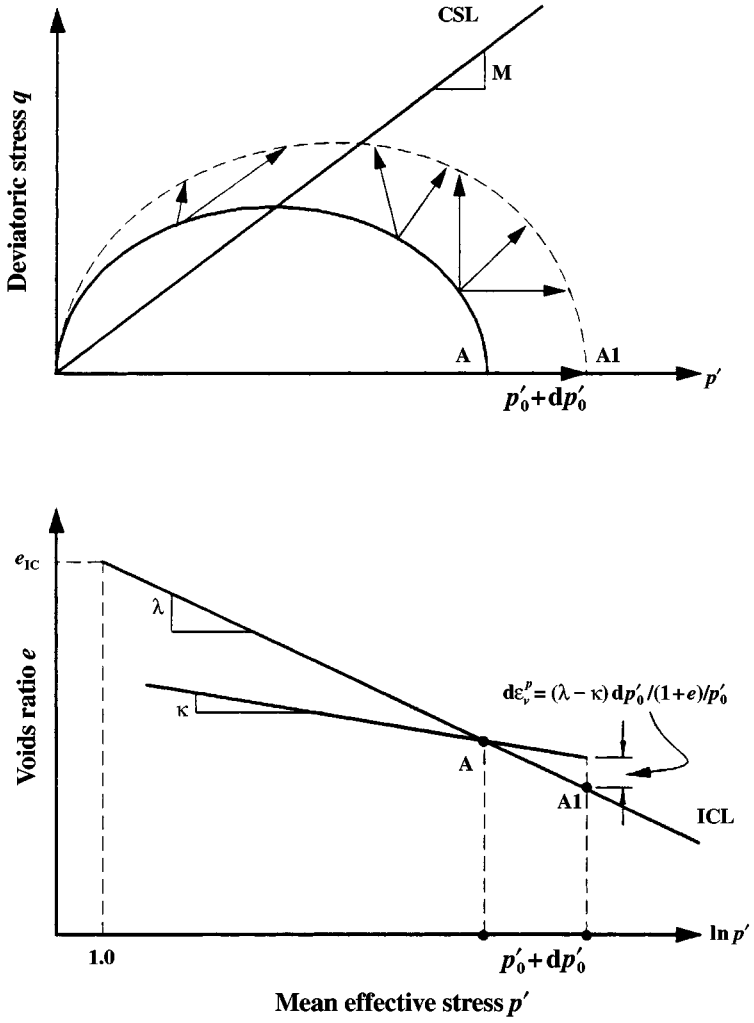

Figure 2. Postulate I: elastic or virgin-yielding material

surface is assumed to be purely elastic. Only when a change in the current stress state results in the expansion of the yield surface does plastic deformation occur.

According to this postulate, the Bauschinger effect is ignored and the idealized soil behaviour is as shown in Figure 2. The gradient of the line representing elastic volumetric deformation has a slope κ on this semi-logarithmic plot. The voids ratio corresponding to unit mean effective stress during virgin yielding is a material constant, e_{IC}. In this case, the current mean stress, p', the voids ratio, e, and the size of the current yield surface, p'_0, are related by

$$e = e_{IC} - \kappa \ln p' - (\lambda - \kappa) \ln p'_0 \tag{5}$$

Consequently, the hardening of soil can be linked with the plastic volumetric deformation, $d\varepsilon_v^p$, as follows:

$$d\varepsilon_v^p = \left(\frac{\lambda - \kappa}{1 + e}\right) \frac{dp'_0}{p'_0} \tag{6}$$

According to Postulate I, soil is idealized as an isotropic hardening material with elastic and virgin-yielding behaviour. The yield surface remains the same for any stress excursion inside the yield surface, and expands isotropically for loading which pushes the yield surface outwards. The plastic volumetric strain increment is dependent only on the magnitude of the size change of the yield surface (Figure 2). This type of material idealization has been adopted most commonly in the early constitutive modelling of both metals and soils.[1,6] As far as soils are concerned, such material idealization is perhaps more suitable for clays than for sands.[7]

3.2. Material idealization II: Sub-yielding and virgin-yielding

The Bauschinger effect is significant and cannot be ignored in situations that involve large stress reversals and cyclic loadings. The occurrence of volumetric expansion during monotonic and cyclic shearing is typical for overconsolidated soils, and it is a feature that should be included in constitutive models of such soils. A second material idealization is now introduced with the aim of describing the cyclic loading and providing a more accurate description of the behaviour of overconsolidated soils.

Consider the introduction of a new surface, described as a pseudo-yield surface. This is a surface in stress space on which the current stress state always remains. The pseudo-yield surface has a similar shape as the virgin yield surface, e.g. if the yield surface is elliptical then the pseudo-yield surface will also be an ellipse with the same aspect ratio. The pseudo-yield surface passes through the origin of the p'–q stress space, and its size is denoted by p'_c (Figure 3). The pseudo-yield surface serves as a mapping quantity to indicate the closeness of the current stress state to the virgin yield surface. It is obviously an ideal parameter for linking the magnitude of any plastic deformation associated with a stress change within the yield surface with that corresponding to virgin yielding.

Postulate II. Soil is idealized as a sub-yielding and virgin-yielding material. Plastic deformation is generally induced by a stress change inside the yield surface, as well as by a stress change originating on the current yield surface and causing it to expand. The former is referred to as sub-yielding, and the latter as virgin yielding. The plastic volumetric deformation for virgin yielding is dependent on the change in size of the yield surface only, and that for sub-yielding is dependent on the kinematic effect of the stress history, the current stress ratio level, as well as the size change of the pseudo-yield surface.

For virgin yielding, the increment of plastic volumetric strain is equal to the virgin deformation compliance, multiplied by the change in size of the virgin yield surface, as indicated in equation (6). For sub-yielding, the increment in plastic volumetric strain is equal to the virgin deformation compliance, multiplied by a factor that includes the influence of the current stress ratio, by a kinetmatic hardening factor α that reflects the effect of stress history, and by the change in size of the pseudo-yield surface, dp'_c. Thus for sub-yielding, $d\varepsilon_v^p$ can

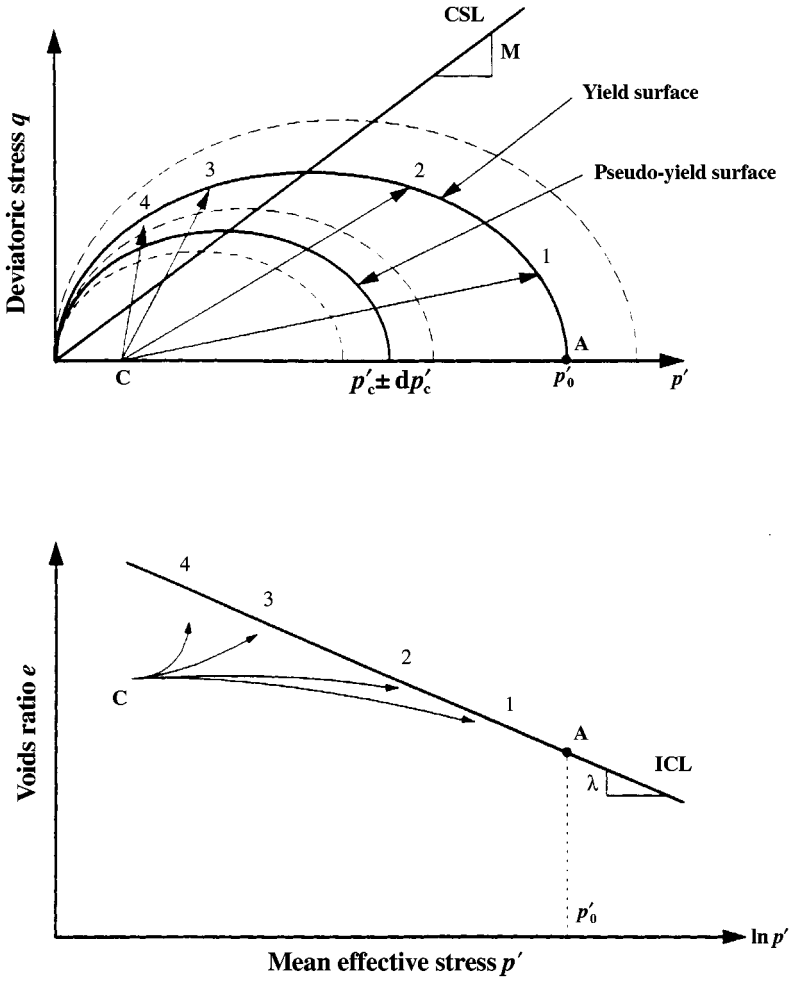

Figure 3. Postulate II: soil behaviour including sub-yielding

be written as

$$d\varepsilon_v^p = \alpha \left(1 - \frac{\eta}{M}\right)\left(\frac{\lambda - \kappa}{1 + e}\right)\frac{dp'_c}{p'_0} \tag{7}$$

where η denotes the current stress ratio (q/p') and M is the critical state stress ratio.

The term $(1 - \eta/M)$ in equation (7) represents the influence of stress ratio on sub-yielding. Consequently, yielding with $dp'_c > 0$ in the low stress ratio range results in volumetric contraction. For yielding with $\eta > M$, volumetric expansive strain occurs if $dp'_c > 0$. When $dp'_c < 0$, the sign of $d\varepsilon_v^p$ will be changed. Comparing equations (6) and (7), it may be seen that the rate of volumetric deformation is continuous for loading from sub-yielding to virgin yielding only for situations with $\eta = 0$.

The parameter α is a function of stress history. Generally, α takes a value between 0 and 1, with $\alpha = 0$ corresponding to purely elastic deformation (i.e. in this case Postulate II reduces to Postulate I), and $\alpha = 1$ corresponding to virgin yielding. In order to describe the Bauschinger effect accurately, the Mroz–Iwan theory of working hardening[8,9] can be used to determine the value of α. A simple scalar expression for α is proposed here, i.e.

$$\alpha = \begin{cases} \left(\dfrac{p'_c - p'_u}{p'_0 - p'_u}\right) & \text{if } dp'_c \geqslant 0 \\ \left(1 - \dfrac{p'_c}{p'_0}\right) & \text{if } dp'_c < 0 \end{cases} \tag{8}$$

in which p'_u is the minimum size of the pseudo-yield surface previously attained, i.e. $p'_u = \min\{p'_c\}$. When the stress state returns to virgin yielding, the memory of the previous loading is lost, and $p'_u = p'_0$. According to equation (8), α represents the kinetmatic hardening effect of a simple stress reversal. During loading, the value of α increases with p'_c, and is equal to 1 when the current stress states returns to the virgin yield surface as previously noted. During unloading, the value of α increases as the stress state moves away from the virgin yield surface.

If there is negligible plastic deformation during unloading, equation (8) can be modified as follows:

$$\alpha = \begin{cases} \left(\dfrac{p'_c - p'_u}{p'_0 - p'_u}\right) & \text{if } dp'_c \geqslant 0 \\ 0 & \text{if } dp'_c < 0 \end{cases} \tag{9}$$

With this modification the soil behaves elastically during unloading, and sub-yielding is a phenomena associated only with reloading inside the virgin yield surface. This type of material idealization has been frequently adopted.[3,4,10,11] For example, Hashiguchi[12] introduced the concept of a sub-yield surface to model the transition from elastic deformation to plastic deformation.

According to Postulate II, soil is idealized as an isotropic-kinematic hardening material with two types of plastic behaviour, sub-yielding and virgin yielding. The virgin yield surface varies isotropically for any plastic volumetric deformation. The soil response during sub-yielding is dependent on kinematic hardening. Both volumetric contraction and expansion can occur in sub-yielding, depending on the stress ratio and the sign of dp'_c. Because plastic volumetric deformation is induced by sub-yielding, the virgin yield surface will also be influenced by sub-yielding. This type of material idealization provides a simplified alternative for modelling the kinematic hardening of soils where an accurate description of the translation of the pseudo-yield surface may be very complicated.

3.3. Material idealization III: Elasticity, sub-yielding and virgin-yielding

When a very large number of cycles of loading is applied to a soil, such as might be imposed rapidly by an earthquake or more slowly by an offshore structure, it is essential to calculate accurately the volumetric response of the soil. If the repeated loading is rapid by comparison with drainage times for the saturated soil, then it may not be possible for the full volumetric response to develop, because of the inability of the pore water to move out of or into the voids of the soil,

i.e. the soil will have insufficient time during the loading to drain fully. In such cases the pore pressure response in each closed cycle of loading is of interest. The development of large positive pore pressures may weaken the soil, the consequences of which may be very important in practice. It is therefore important to be able to model the tendency for the soil to change the viods ratio, during repeated loading, especially if the accumulation of permanent volumetric strain is prohibited by the drainage conditions and the rapidity of loading.

There have been many attempts to develop soil models to predict the behaviour under cyclic loading, ranging from those that are mechanically and mathematically more rigorous, usually requiring a detailed analysis of each individual cycle,[3,13] to the more approximate theories that take a phenomenological view of the development of permanent strain and pore water pressure.[14,15] From a practical viewpoint it will almost certainly be necessary to sacrifice some rigor so that numerical solution of complicated boundary value problems, involving perhaps thousands or even millions of cycles, remains feasible.

The classic Mroz–Iwan theory also has deficiencies for cyclic loading such as: (1) the theory predicts no permanent plastic strain for loading along a closed stress path, and (2) it normally does not differentiate the influence of shearing and consolidation. Hence a third material idealization is proposed to deal with these cases.

Postulate III. Soil is idealized as a material that exhibits three possible modes of deformation: elasticity, sub-yielding, and virgin yielding. There exists a small elastic region in stress space which kinematically follows the current stress state; only elastic deformation is produced for a stress change inside this zone. Virgin yielding is produced for a change in stress state originating on the current yield surface and causing it to expand. Sub-yielding is produced for a stress change located inside the yield surface and outside the elastic zone.

The shape and size of the elastic region can be determined from experimental results. It is convenient to assume that it has the same shape as the yield surface, and follows the current stress state in such a way as to remain tangential to the pseudo-yield surface at the current stress point. The size of the elastic zone p'_e can be expressed as a fraction of the virgin yield surface, i.e. $p'_e = \beta p'_0$. If $\beta = 0$, there is no elastic zone.

The elastic volumetric strain is equal to the elastic deformation compliance $(\kappa/p'(1+e))$ multiplied by the change in mean effective stress dp'. During virgin yielding, the incremental plastic volumetric strain is equal to the virgin deformation compliance, $((\lambda-\kappa)/p'_0(1+e))$, multiplied by the change in size of the yield surface dp'_0 as expressed in equation (6).

Sub-yielding occurs for stress change inside the virgin yield surface and outside the elastic zone. After examining both qualitatively and quantitatively a large body of experimental data, which includes cyclic loading tests with constant stress ratio,[16,17] and some from more general cyclic shearing,[18–22] the following mathematical expression for the overall plastic volumetric strain increment is proposed:

$$d\varepsilon_v^p = \Delta \left\{ \left(\frac{1}{N^{2/3}} \right) \left(\frac{\alpha(\lambda-\kappa)}{(1+e)\,p'_0} \right) \sqrt{dp'^2 + dq^2} \right\} \tag{10}$$

in which

$$\Delta = l_1 \left(\frac{\sigma'_3}{\sigma'_1} \right) \frac{dp'}{\sqrt{dp'^2 + dq^2}} + l_2 \sqrt{\frac{dq^2}{dp'^2 + dq^2}} \left(\frac{\sigma'_1}{\sigma'_3} \right)^{n_1} \sin\left(\frac{\eta}{M}\,\pi \right) \tag{11}$$

Δ is made up of two parts. The first part is contributed by a change in the mean stress and the sign of the volumetric strain increment is the same as dp'. The second part is contributed by a change in the deviatoric stress, and the sign of the volumetric strain increment is dependent on η/M only, irrespective of the sign of dq. Generally speaking, the rate of the volumetric deformation with respect to a stress quantity is not continuous during the transition from sub-yielding to virgin yielding.

l_1 and l_2 are soil parameters. The influence of these two parameters can be separated by considering the separate cases where $dp' = 0$ and $dq = 0$. In this way the values of l_1 and l_2 can be decided independently and directly from tests.

The parameter n_1 is dependent on the dilative nature of the soil. It is assumed that for clays $n_1 = 1$, and for strongly dilative sand $n_1 = 2$.

N is the number of cycles of loading, and clearly it is not a direct soil parameter. Strictly speaking, the influence of repeated cycles of loading should be reflected through internal soil variables. However, to avoid excessive complexity in the formulation of the soil model and to reflect the trends observed in cyclic loading experiments, N is included in the model formulation. This can be regarded as an expedient and pragmatic approach to dealing with the problem of modelling the response of a granular medium to repeated applications of loading.

A precise mathematical definition of N, which is both consistent and applicable to loadings along general stress paths, is actually very complicated. Although there is large amount of information in geotechnical engineering expressed in terms of N,[23] it appears to the authors that a suitable general definition is not currently available. The authors plan to address this problem and examine the applicability of a general definition for N for some dynamic geotechnical problems in a future paper. For this paper, only the repeated loadings where the number of cycles can be accounted by the traditional method[3] are of concern. It is suggested that N should be set equal to 1 for the first cycle of loading following each episode of virgin yielding.

α has the same physical meaning as that assumed in Postulate II, and its value can be determined in the manner described previously. In order to employ parameter α in situations that involve a large number of cycles of loading, a new approximation for the Mroz–Iwan theory is required, as proposed in the following paragraphs.

Suppose a soil is firstly loaded from stress state O to A, then, is unloaded to B. After that, the soil is subjected to uniform cyclic loding between B and C (Figure 4). According to the Mroz–Iwan theory, a schematic representation of the translation of the previously encountered yield surfaces in the cyclic loding is shown in Figure 4. For cyclic loading along BC, only yield loci inside a certain surface y_4 may be affected. y_4 is the minimum yield surface which contains the stress path BC. This set of yield loci inside y_4 will be translated repeatedly between points B and C as the stress state repeatedly traces the vector BC. Hence, in this case a modification to the factor α is proposed to incorporate the effects of kinematic hardening.

For the case of loading from B to C in a stress cycle, where the current stress state can be represented by point D on the line BC, α is determined from

$$\alpha = \begin{cases} \left(\dfrac{p'_c - p'_u}{p'_0 - p'_u}\right) \approx \left(\dfrac{p'_4}{p'_0 - p'_e}\right)\left(\dfrac{\| \mathrm{BD} \| - \| \mathrm{BE} \|}{\| \mathrm{BC} \|}\right) & \text{if } p'_c > p'_e \\ 0 & \text{if } p'_c \leqslant p'_e \end{cases} \tag{12}$$

where p'_4 is the size of yield surface y_4, and E is the point where the stress state reaches the elastic boundary after transversing it from point B. It is easy to show that the distance from B to D is

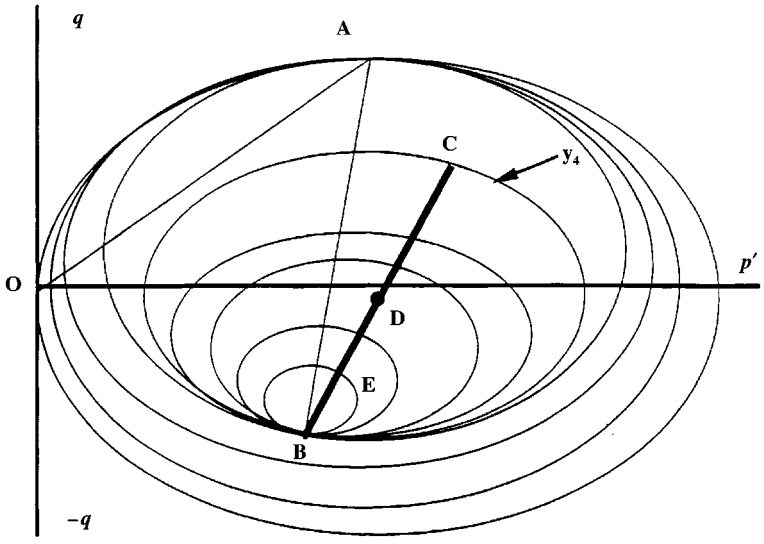

Figure 4. Kinematic transition of yield surfaces during cyclic loading according to Mroz–Iwan theory

given by

$$\| \mathrm{BD} \| = \sqrt{(p'_{\mathrm{D}} - p'_{\mathrm{B}})^2 + (q_{\mathrm{D}} - q_{\mathrm{B}})^2} \tag{13}$$

The distances from B to C and B to E can be determined from formulae similar in form to equation (13). Thus, using equations (12) and (13), the precise determination of the complete nest of yield loci and their associated translations is avoided. This approach has obvious computational advantages.

In Postulate III, soil is idealized as a material that exhibits elasticity, sub-yielding and virgin-yielding with isotropic and kinematic hardening. When the stress state turns inside the elastic zone in a stress reversal, purely elastic behaviour will be observed. For one closed cycle of loading, residual plastic volumetric strain is normally induced. Its magnitude is inversely proportional to the numer of cycles, and the size of the virgin yield surface. The nature of the plastic volumetric strain, compressive or expansive, is dependent on the current stress ratio only. The virgin yield surface varies during subsequent loading. The rate of volumetric strain, i.e. $\mathrm{d}\varepsilon_{\mathrm{v}}/\mathrm{d}p'_{\mathrm{c}}$, generally is not continuous during the transition from sub-yielding to virgin yielding.

The following expression is proposed for the general plastic strain increment under sub-yielding with $\mathrm{d}p'_{\mathrm{c}} \geqslant 0$:

$$\mathrm{d}\varepsilon^p_{ij} = \left[\frac{3\,(\sigma'_{ij} - p'\delta_{ij})}{Mp'} + \frac{\Delta}{3}\,\delta_{ij} \right] \frac{1}{N^{2/3}}\,\frac{\alpha(\lambda - \kappa)}{(1+e)}\,\frac{\sqrt{\mathrm{d}p'^2 + \mathrm{d}q^2}}{p'_0} \tag{14}$$

A basic reason for adopting equation (14) is the assumption that the deviatoric plastic strain increment resulting from shearing is proportional to the current deviatoric stress. This assumption has been verified by Liu,[7] using an extensive body of test data, mostly for sand.

4. IMPLEMENTATION IN CONSTITUTIVE MODELS

The three postulates described in the previous section provide different idealizations of the mechanical behaviour of reconstituted soil. They are largely based on physical reasoning and contain varying degrees of complexity. They can be implemented quite easily into most constitutive models that include volumetric-strain-controlled hardening. A detailed example is given here to demonstrate how the implementation is achieved. The well-known modified Cam Clay model is chosen for its clear physical basis and simplicity.

4.1. Summary of the Modified Cam Clay model

Details of the modified Cam Clay model can be found in Reference 24. The essential features of the model can be summarized in the following four points.

4.1.1. Elasticity. The elastic deformations can be expressed in terms of the consolidation constant κ and Poisson's ratio v, i.e.

$$\mathrm{d}\varepsilon_{\mathrm{v}}^{\mathrm{e}} = \left(\frac{\kappa}{1+e}\right)\frac{\mathrm{d}p'}{p'} \tag{16}$$

$$\mathrm{d}\varepsilon_{\mathrm{d}}^{\mathrm{e}} = \frac{2(1+v)}{9(1-2v)}\left(\frac{\kappa}{1+e}\right)\frac{\mathrm{d}q}{p'} \tag{17}$$

in which $\mathrm{d}\varepsilon_{\mathrm{v}}^{\mathrm{e}}$ and $\mathrm{d}\varepsilon_{\mathrm{d}}^{\mathrm{e}}$ represent the elastic increments of volumetric and deviatoric strain.

4.1.2. Yield surface. An elliptical yield surface is assumed in the model, and it has the following expression:

$$f = \left(\frac{q}{0{\cdot}5\,Mp'_0}\right)^2 + \left(\frac{p' - 0{\cdot}5\,p'_0}{0{\cdot}5\,p'_0}\right)^2 - 1 = 0 \tag{18}$$

where M is the stress ratio at critical state.

4.1.3. Flow law. Associated plastic flow is assumed so that the yield surface is also the plastic potential, g, i.e.

$$g = f \tag{19}$$

4.1.4. Hardening law. Hardening is governed by the plastic volumetric strain, such that

$$\frac{\mathrm{d}p'_0}{p'_0} = \left(\frac{1+e}{\lambda-\kappa}\right)\mathrm{d}\varepsilon_{\mathrm{v}}^{\mathrm{p}} \tag{20}$$

4.2. Modified Cam Clay incorporating Postulate I

The material idealization in Postulate I is the same as that in the conventional modified Cam Clay model, and therefore, no modification to the stress–strain relationship is required. The following incremental forms for the stress–strain relationships can be obtained.

4.2.1. Virgin yielding. The total strain is made of elastic and plastic parts, so that

$$d\varepsilon_v = d\varepsilon_v^e + d\varepsilon_v^p = \left(\frac{\kappa}{1+e}\right)\frac{dp'}{p'} + \left(\frac{\lambda-\kappa}{1+e}\right)\frac{dp'_0}{p'_0} \tag{21}$$

and

$$d\varepsilon_d = d\varepsilon_d^e + d\varepsilon_d^p = \frac{2(1+v)}{9(1-2v)}\left(\frac{\kappa}{1+e}\right)\frac{dq}{p'} + \left(\frac{2\eta}{M^2-\eta^2}\right)\left(\frac{\lambda-\kappa}{1+e}\right)\frac{dp'_0}{p'_0} \tag{22}$$

4.2.2. Subsequent loading. Only elastic deformation takes place during unloading and subsequent loading inside the virgin yield surface. For this condition the strains may be computed from equations (16) and (17).

4.3. Modified Cam Clay incorporating Postulate II

In Postulate II, virgin yielding behaviour is the same as in Postulate I and the corresponding strain increments are given by equations (21) and (22).

During sub-yielding, plastic deformation takes place. The plastic volumetric strain is dependent on the change in size of the pseudo-yield surface. The total volumetric strain increment can be written as

$$d\varepsilon_v = \left(\frac{\kappa}{1+e}\right)\frac{dp'}{p'} + \alpha\left(\frac{M-\eta}{M}\right)\left(\frac{\lambda-\kappa}{1+e}\right)\frac{dp'_c}{p'_0} \tag{23}$$

The value of α is determined by equation (8) or by equation (9).

To calculate the magnitude of plastic strain increments, the direction of the plastic strain increment must first be determined. The direction of the plastic strain increment for reloading, i.e., $dp'_c > 0$, is assumed to be normal to the pseudo-yield surface, so that

$$\frac{d\varepsilon_v^p}{d\varepsilon_d^p} = \frac{M^2-\eta^2}{2\eta} \tag{24}$$

Consequently, for monotonic loading, the distortional strain increment can be expressed as

$$d\varepsilon_d = \frac{2(1+v)}{9(1-2v)}\left(\frac{\kappa}{1+e}\right)\frac{dq}{p'} + \alpha\left(\frac{2\eta}{M(M+\eta)}\right)\left(\frac{\lambda-\kappa}{1+e}\right)\frac{dp'_c}{p'_0} \tag{25}$$

For a closed cycle of stress change involving monotonic unloading and reloading, it is widely observed that there is a profound Bauschinger effect for the deviatoric strain. Equation (24) indicates the plastic deviatoric strain increment is proportional to the current stress ratio. This prediction is not consistent with the observed Bauschinger phenomenon. The following equation for distortional strain increment for unloading, i.e. $dp'_c < 0$, is proposed:

$$d\varepsilon_d = \frac{2(1+v)}{9(1-2v)}\left(\frac{\kappa}{1+e}\right)\frac{dq}{p'} + \alpha\left(\frac{2(\eta_u-\eta)}{M(M+\eta)}\right)\left(\frac{\lambda-\kappa}{1+e}\right)\frac{dp'_c}{p'_0} \tag{26}$$

where η_u is the stress ratio at which unloading occurs. It may be noticed that the plastic part of $d\varepsilon_d$ calculated from equation (26) is negative for unloading.

4.4. *Modified Cam Clay incorporating Postulate III*

In Postulate III, virgin-yielding behaviour is the same as that in Postulates I and II, and the corresponding strain increments are as given by equations (21) and (22).

Inside the virgin yield surface there are two distinct deformation zones. In the truly elastic zone, the strain increments can be calculated from equations (16) and (17). The elastic zone is bounded by an ellipse and covers the following area in stress space

$$\left(\frac{q-q_e}{0{\cdot}5\,M\,\beta p'_0}\right)^2+\left(\frac{p'-p'_e}{0{\cdot}5\,\beta\,p'_0}\right)^2-1\leqslant 0 \tag{27}$$

where $(p'_e,\ q_e)$ is the centre of the ellipse defining the elastic zone, and β is a soil parameter, indicating that the size of the elastic zone as a fraction of the size of the virgin yield surface.

For sub-yielding, the total volumetric strain is equal to the elastic part, plus the plastic parts expressed in equation (10), i.e.

$$d\varepsilon_v=\left(\frac{\kappa}{1+e}\right)\frac{dp'}{p'}+\left\{l_1\left(\frac{\sigma'_3}{\sigma'_1}\right)dp'+l_2\sqrt{dq^2}\left(\frac{\sigma'_1}{\sigma'_3}\right)^{n_1}\sin\left(\frac{\eta}{M}\pi\right)\right\}\left(\frac{\alpha(\lambda-\kappa)}{(1+e)}\right)\left(\frac{1}{N^{2/3}}\right)\frac{1}{p'_0} \tag{28}$$

According to expression (14), the deviatoric strain for subyielding with $dp'_c\geqslant 0$ is

$$d\varepsilon_d=\frac{2(1+v)}{9(1-2v)}\left(\frac{\kappa}{1+e}\right)\frac{dp'}{p'}+\left(\frac{2\eta}{M}\right)\left(\frac{1}{N^{2/3}}\right)\left(\frac{\alpha(\lambda-\kappa)}{(1+e)}\right)\frac{\sqrt{dp'^2+dq^2}}{p'_0} \tag{29}$$

The deviatoric strain increment for loading with $dp'_c<0$ is determined by the following equation:

$$d\varepsilon_d=\frac{2(1+v)}{9(1-2v)}\left(\frac{\kappa}{1+e}\right)\frac{dp'}{p'}-\left(\frac{2(\eta_u-\eta)}{M}\right)\left(\frac{1}{N^{2/3}}\right)\left(\frac{\alpha(\lambda-\kappa)}{(1+e)}\right)\frac{\sqrt{dp'^2+dq^2}}{p'_0} \tag{30}$$

where η_u is the stress ratio at which η decreases. Negative plastic distortional strain increments are valid.

5. APPLICATIONS

In order to evluate the three postulates, various versions of the modified Cam Clay models incorporating the three postulates were implemented in numerical procedures, and these were used to simulate the response of single soil elements subjected to various stress paths. Four sets of simulations are presented here. They investigate the behaviour of ideal soil samples subjected to the following stress conditions:

1. isotropic loading and unloading,
2. monotonic compression of specimens with different initial overconsolidation ratios,
3. lightly overconsolidated soil subjected to cyclic triaxial loading, and
4. a large number of cycles of deviatoric loading applied to heavily overconsolidated soil.

In all the simulations, one set of soil parameters was adopted, as listed in Table I.

Table I. Model parameters

Postulate	M	λ	κ	e_{IC}	ν	β	l_1	l_2	n_1
I	1·20	0·16	0·05	2·176	0·25	—	—	—	—
II	1·20	0·16	0·05	2·176	0·25	—	—	—	—
III	1·20	0·16	0·05	2·176	0·25	0	0·6	0·35	2

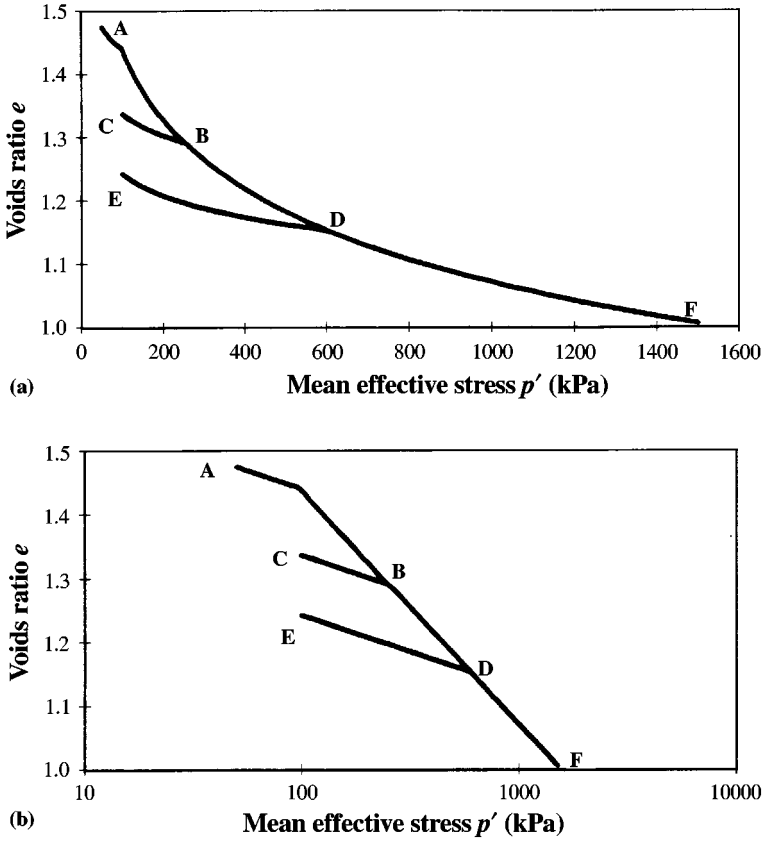

Figure 5. Soil behaviour under cyclic isotropic loading predicted via Postulate I

For Postulate III, $\beta = 0$ has been selected, so that the ideal soil exhibits no purely elastic behaviour. Four additional soil parameters are required for soil models that incorporate Postulate III. In the examples considered here, the behaviour of strongly dilative soil is considered, and therefore, n_1 has been set at the value of 2.

5.1. *Isotropic loading and unloading*

In this example the initial stress state is isotropic with $p' = 50$ kPa and the initial voids ratio is $e = 1{\cdot}474$ (denoted by point A in Figures 5–7), which gives the size of the virgin yield surface as

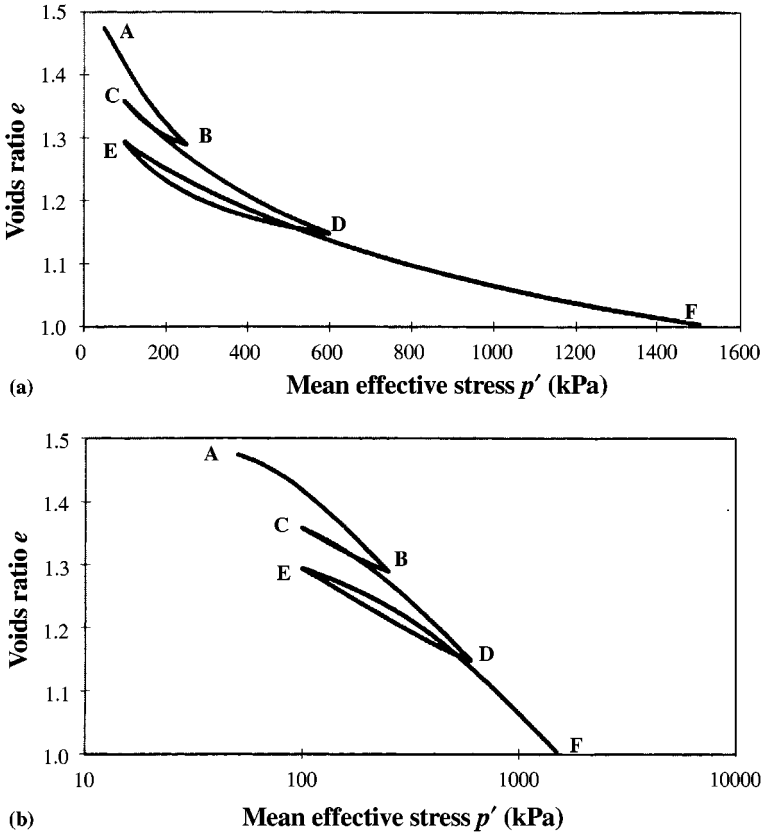

Figure 6. Soil behaviour under cyclic isotropic loading predicted via Postulate II

$p'_0 = 100$ kPa, which means that the soil originally has an OCR of 2. The isotropic stress path applied to the element of soil is defined as follows: an increase to $p' = 250$ kPa (point B), followed by a reduction to $p' = 100$ kPa (point C), another increase to $p' = 600$ kPa (point D), another reduction to $p' = 100$ kPa (point E), and finally an increase to $p' = 1500$ kPa (point F).

Predictions by the three models of the volumetric response of the soil to this form of loading and unloading are shown in Figures 5–7. Both natural and logarithmic scales for p' have been used to plot the predictions. Experimental data for a consolidation test on reconstituted Kaolin clay[25] are shown in Figure 8 for comparison. The material idealization for Postulate I is clearly seen in Figures 5(a) and (b). The two zones, elasticity and virgin yielding, are sharply divided. The predicted responses provided by Postulates II and III successfully capture the Bauschinger effect. For Postulate II, there is a smooth transition between sub-yielding and virgin-yielding, although a rapid change in soil stiffness around the transmission can still be observed.

5.2. *Monotonic shearing*

Three different monotonic stress paths have been analysed; it is assumed that in all three tests the size of the initial virgin yield surface is given by $p'_0 = 200$ kPa. Each specimen was then

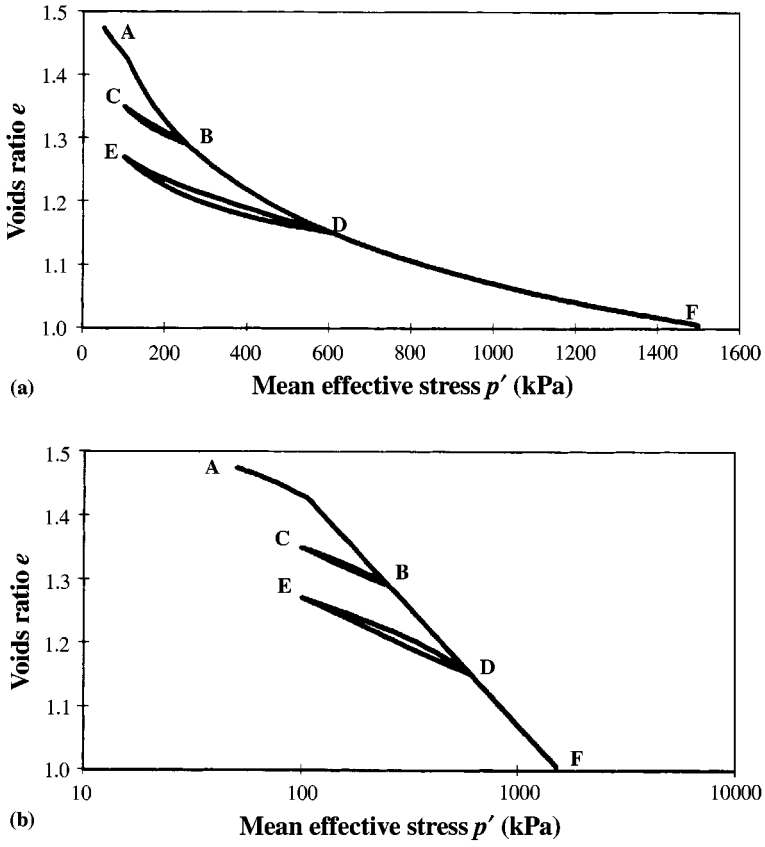

Figure 7. Soil behaviour under cyclic isotropic loading predicted via Postulate III

subjected to a conventional drained triaxial compression test with a constant confining pressure. The initial stress states prior to shearing are isotropic and are as follows: $p' = 33{\cdot}3$, 150 and 200 kPa for specimens A, B, and C, respectively. As a result, the initial voids ratios for the three cases are 1·418, 1·343 and 1·329, respectively. The OCRs were 6, 1·33 and 1 for specimens A, B and C, respectively.

Predictions of the behaviour during the shearing phase of each test are of interest, for which the stress path can be described by $dq/dp' = 3$. Results of the numerical simulations are shown in Figures 9–11. Included in these figures are indications of the stress paths, predictions of the changes in voids ratio, as well as the predicted stress–strain relationships. Also plotted in some figures, for reference purposes, is the critical state line. Typical data of reconstituted Bothkennar clay under shearing are shown in Figure 12. They were drained triaxial compression tests on four samples. The OCRs for the four samples were 1, 1·14, 1·33, 2, and 4. It should be noticed that the initial stress states for all the four tests were anisotropic (for details see Allman & Atkinson, 1992).

Modified Cam Clay with Postulate I behaves elastically within the virgin yield surface (Figure 9). For specimen A, purely elastic deformation is seen for path A-1. At point 1, the peak strength is reached. Beyond the peak, the soil softens along path 1–2. For test B, a purely elastic

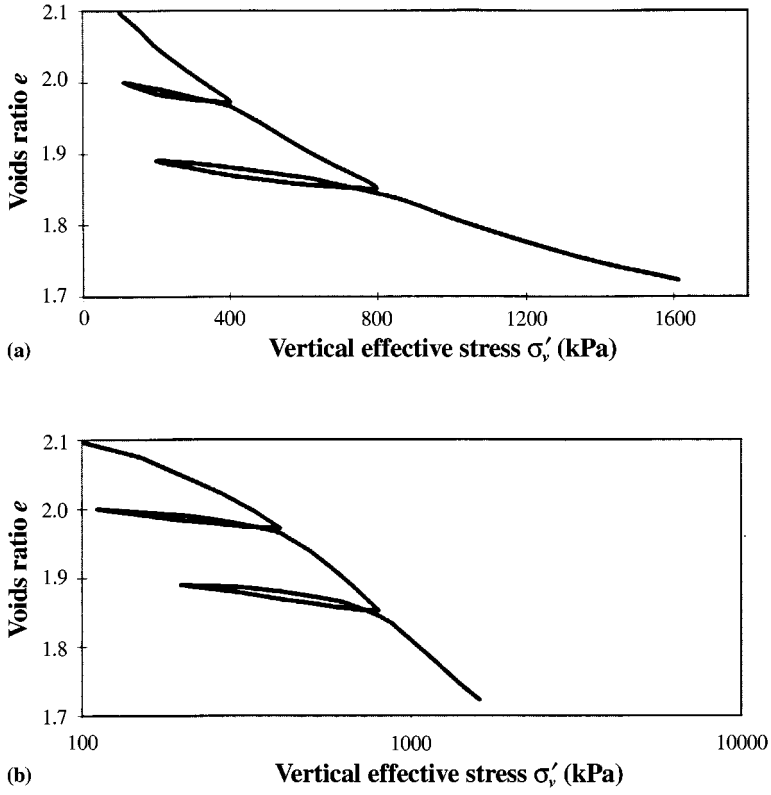

Figure 8. The behaviour of remoulded Kaolin clay in an oedometer test (Test data after Butterfield and Baligh[25])

region B-3 is seen. At stress state 3, yielding starts, and thereafter a sharp drop in stiffness is seen. For test C, virgin yielding occurs throughout the loading. Only compressive volumetric strain is seen for test B and C. Expansive volumetric strain is seen for test A only after soil starts to soften. The stiffness of sample A is far greater than that of samples B and C. Sample A finally softens to the critical state strength after a large distortional strain. In all tests the stress states and voids ratios of the samples end up on the critical state line.

For the model with Postulate II (Figure 10), plastic deformation occurs for loading inside the virgin yield surface. This means that the stiffness of the soil inside the virgin yield surface is modified, and is dependent on the value of OCR. A specimen with a higher OCR subjected to a conventional drained triaxial test undergoes less volumetric compression. Qualitatively, the predictions from Postulate III are the same as those from Postulate II for virgin yielding and for reloading in the first cycle (Figure 11). As both postulates link the plastic volumetric strain in sub-yielding with the current stress ratio, the peak strength predicted is thus not only dependent on the initial void ratio, but also on the stress path, i.e. the peak strength depends on the voids ratio change and the stress level change accumulated in the test. Dilatancy during sub-yielding for heavily overconsolidated soil is observed, with its magnitude also dependent on OCR, stress ratio, and stress path. This type of behaviour has been observed in physical experiments on soil, as reported in the literature.[20,26,27]

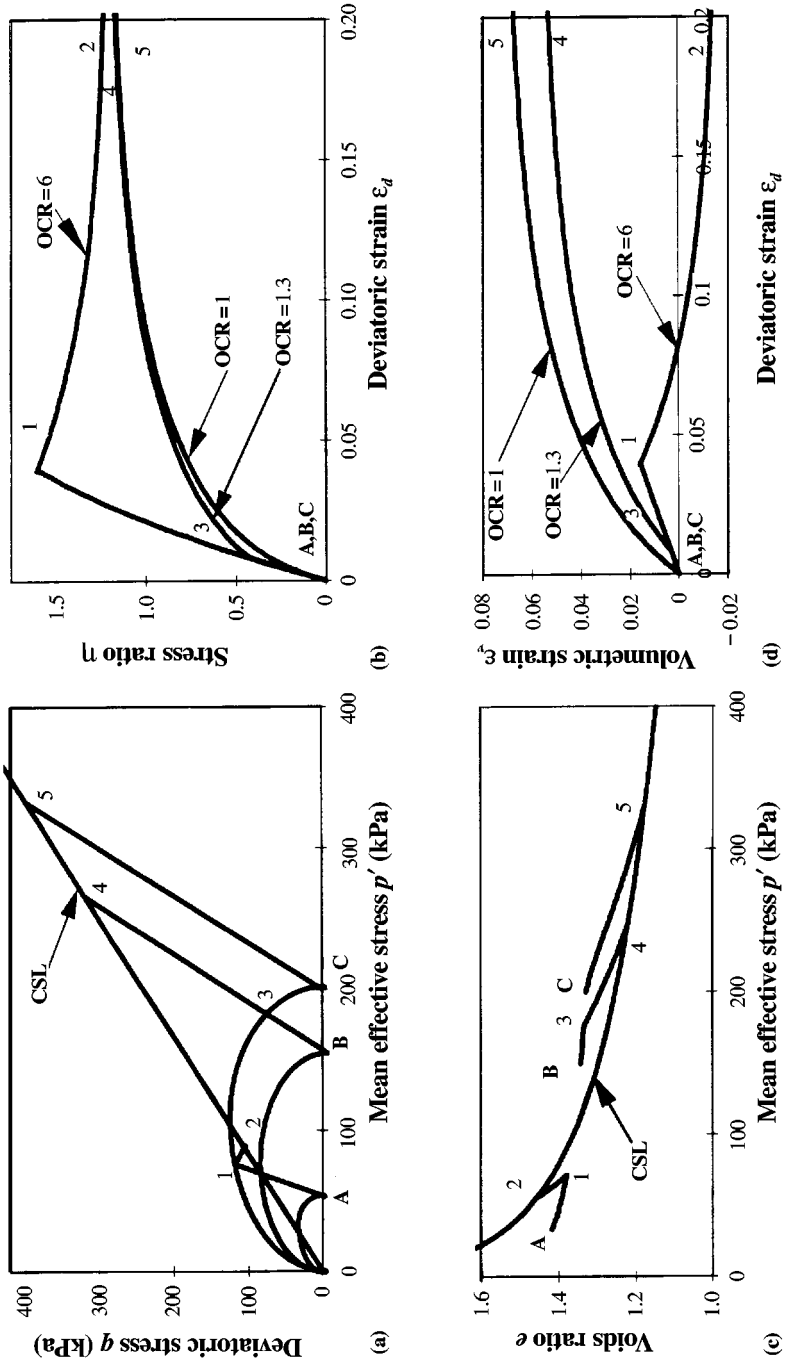

Figure 9. Soil behaviour under monotonic shearing with different OCRs predicted via Postulate I

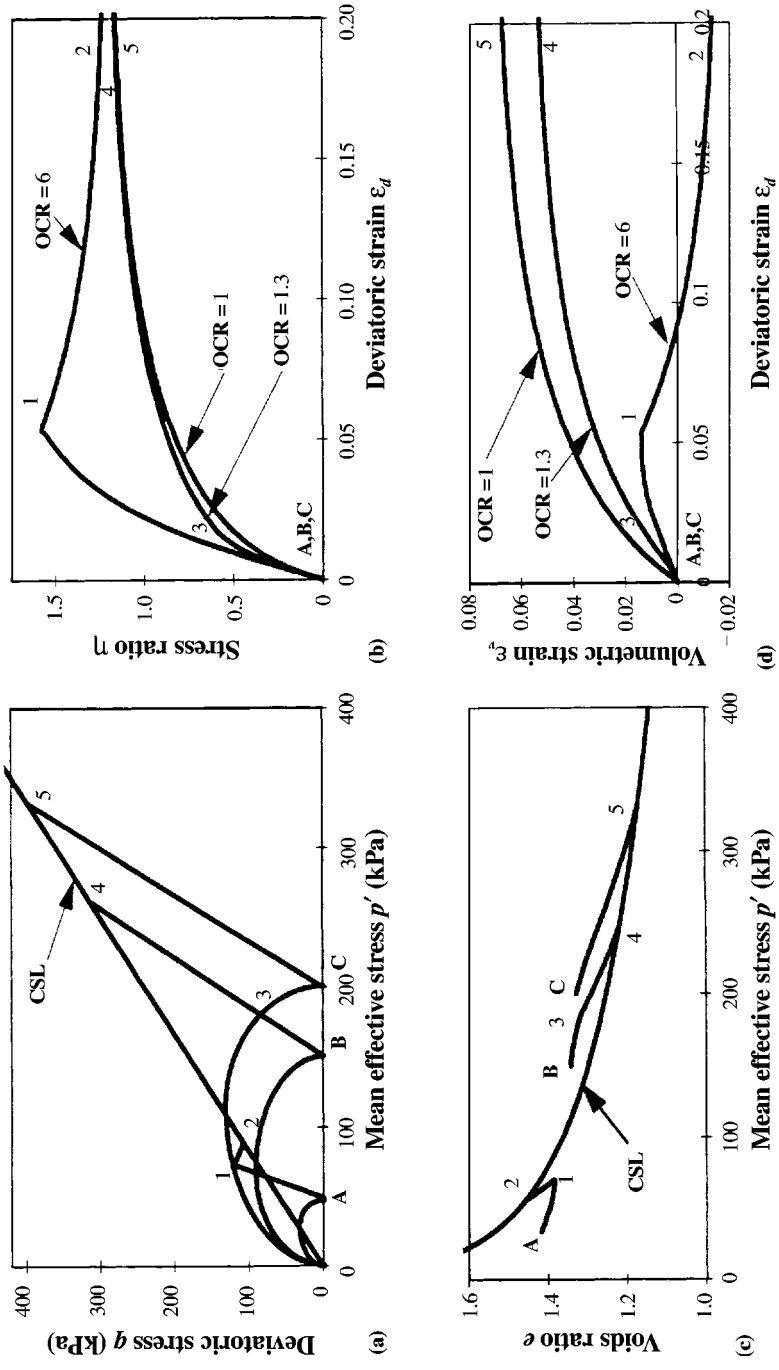

Figure 10. Soil behaviour under monotonic shearing with different OCRs predicted via Postulate II

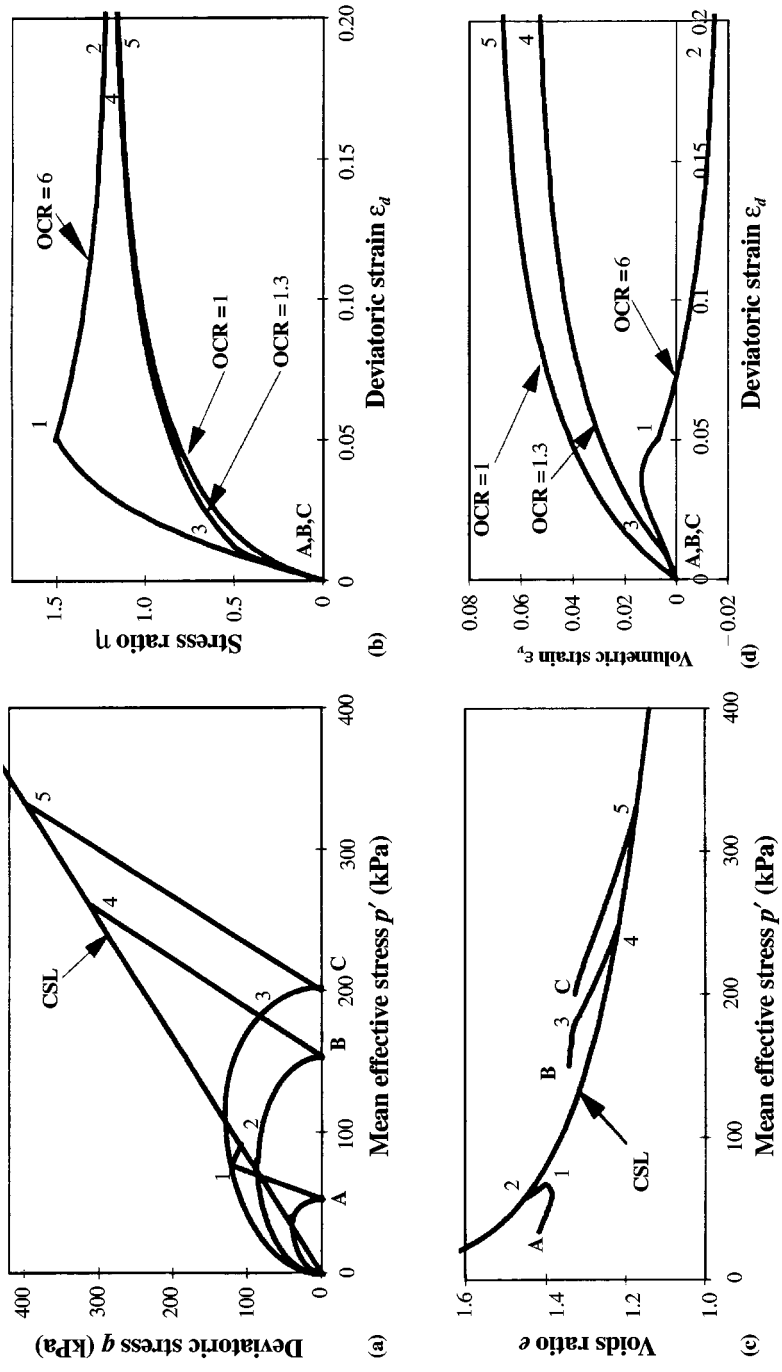

Figure 11. Soil behaviour under monotonic shearing with different OCRs predicted via Postulate III

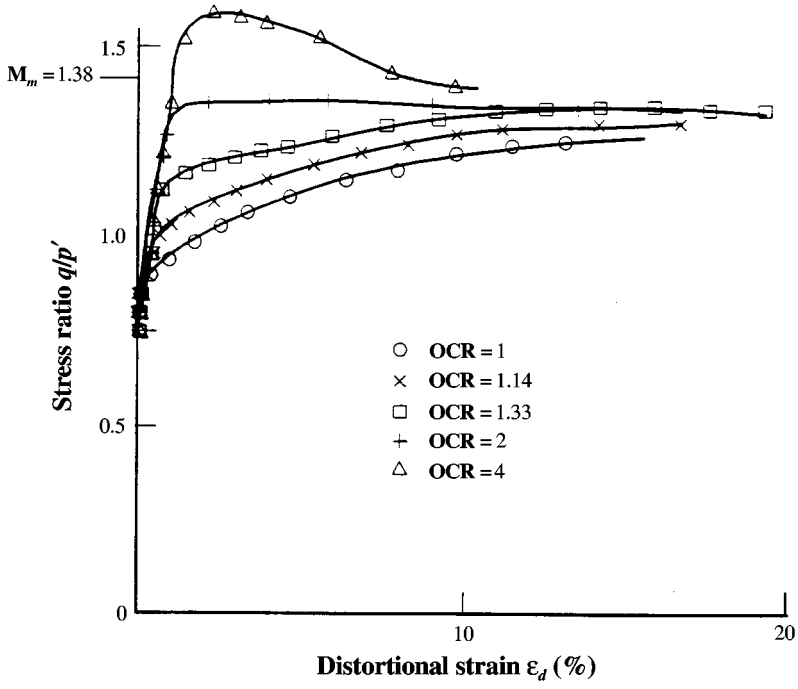

Figure 12. The behaviour of a remoulded clay under drained triaxial tests (Test data after Allman and Atkinson)

It has long been observed that both the original Cam Clay model and the modified Cam Clay model have the deficiency that the peak strength for heavily overconsolidated soil is overestimated.[13,27] Because for heavily overconsolidated soil expansive plastic volumetric strain is predicted by Postulates II and III, the yield surface will shrink for subsequent yielding, and the peak strengths predicted by the two postulates are reduced. In the above case for sample A, the peak frictional angles predicted are 39·4° for Postulate I, 38·7° for Postulate II, and 37° for Postulate III.

These examples demonstrate that Postulate I gives good description for soil behaviour in virgin yielding and also a simple and approximate estimation of soil behaviour in subsequent loading. These examples also demonstrate that Postulates II and III represent successfully the subyielding of reconstituted soil. The characteristic differences between heavily overconsolidated soil, lightly overconsolidated soil, and normally consolidated soil are adequately modelled. Expansive plastic volumetric strain is predicted for heavily overconsolidated soil. There is also improvement in representing the peak strength for heavily overconsolidated soil for the models implemented with Postulates II and III.

5.3. Non-uniform cyclic shearing

In this set of calculations the behaviour of lightly overconsolidated soil subjected to several cycles of non-uniform cyclic loading has been predicted. The initial state, state A, for the soil specimens described here is isotropic with $p' = 150$ kPa and $e = 1{\cdot}343$. The initial virgin yield

surface is thus defined by $p'_0 = 200$ kPa. The applied stress path corresponds to a cyclic triaxial test that follows a conventional drained stress path with the confining pressure being constant. The soil specimen was firstly loaded to stress state B with $p' = 200$ kPa and $q = 150$ kPa. It was then unloaded to C, where $p' = 150$ kPa, $q = 0$, and reloaded to D, where $p' = 225$ kPa and $q = 225$ kPa. After that, the soil specimen was unloaded to E, with $p' = 210$ kPa, $q = 180$ kPa, and reloaded to F, with $p' = 240$ kPa and $q = 270$ kPa. Finally, the soil was unloaded to G, with $p' = 150$ kPa, $q = 0$, i.e. the initial stress state, before being loaded to failure.

The results of the simulation that incorporate Postulate I are shown in Figure 13(a), where the stress ratio has been plotted against the distortional strain, and in Figure 13(b) which shows a plot of volumetric strain versus stress ratio. Simulations that correspond to Postulates II and III are shown in Figures 14 and 15, respectively. Typical data of soil behaviour during non-uniform cyclic loading are shown in Figure 16 for River Welland sand[28] and Figure 17 for Fuji sand.[18]

The different material idealizations are clearly reflected in the numerical simulations. The simplification of purely elastic behaviour inside the virgin yield surface (Postulate I) is seen in both Figures 13(a) and 13(b), where (1) the deformation of soil inside the yield surface is recoverable and (2) the yield surface remains the same for loading inside the yield surface. The Bauschinger effect and its variation with different stress paths can be observed in the numerical simulations that incorporate Postulates II and III. The yield surface also varies with subsequent loading.

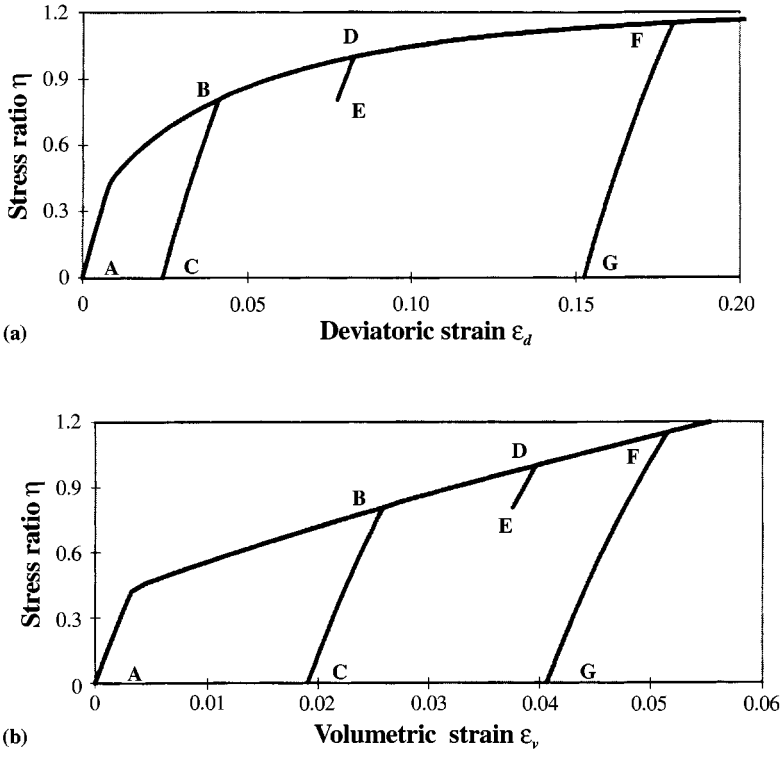

Figure 13. Soil behaviour during non-uniform cyclic loading predicted via Postulate I

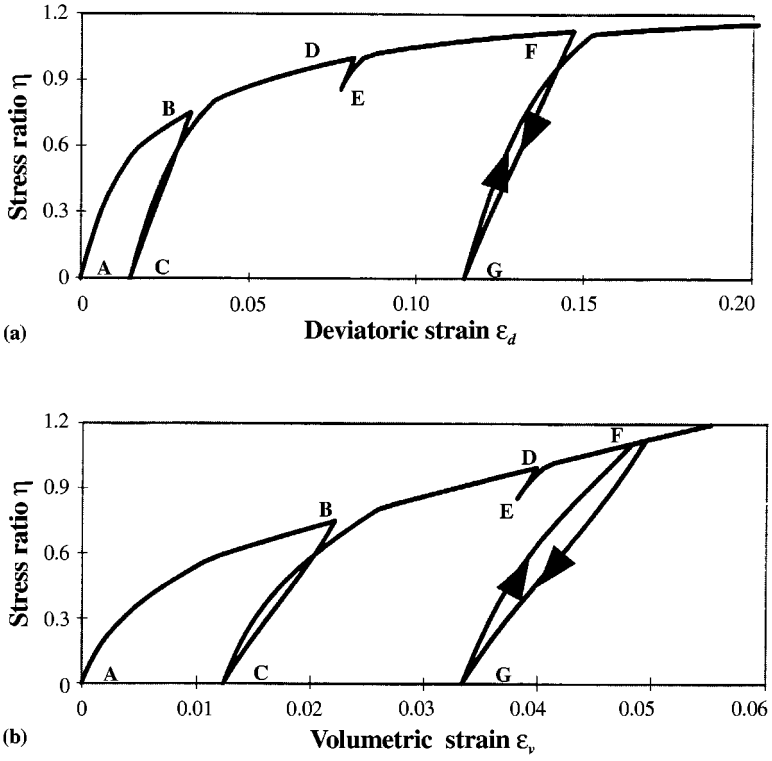

Figure 14. Soil behaviour during non-uniform cyclic loading predicted via Postulate II

For the Postulates II and III, the strain is found to be approximately recoverable for a cyclic loading that involves only a small change in stress, as is seen in stress change along DEF. This feature of the predictions is entirely consistent with observed soil behavior (see Figure 16).

The prediction via Postulate III shows that the volumetric deformation increases continuously during cyclic shearing, though there is a profound Bauschinger effect for deviatoric strain. This feature of soil behaviour has been widely reported, and it has been known that cyclic shearing of soil, particularly granular materials, is a very effective way to change its density.[19–21,29] It is also seen in the prediction that the original lightly overconsolidated soil is changed into a heavily overconsolidated soil, i.e. it has a peak strength and has a softening behaviour, due to the densification arising from the cyclic shearing.

5.4. Uniform cyclic loading

To demonstrate the predictions of soil behaviour under a large number of cycles, three sets of numerical simulations are presented. Because only Postulate III has the capacity to represent reasonably well the behaviour of soil over a large number of repeated load cycles, it is the only one used to predict the cyclic behaviour. In the presentation of these predictions the following notation has been adopted. η_m is the average stress ratio for a stress cycle and η_d is the amplitude

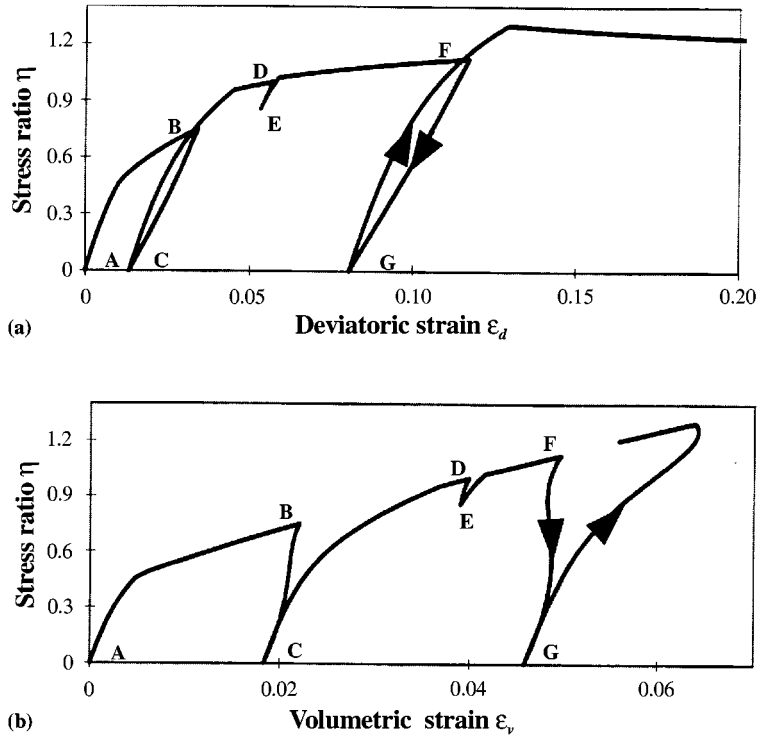

Figure 15. Soil behaviour during non-uniform cyclic loading predicted via Postulate III

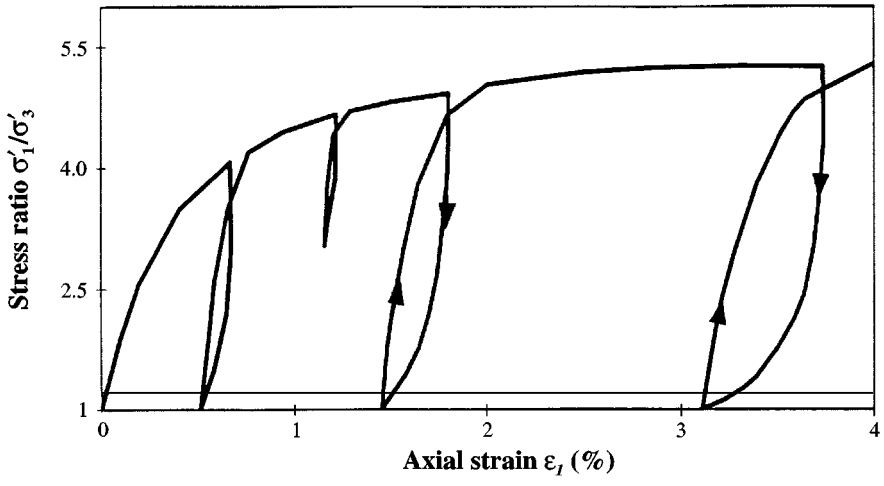

Figure 16. The behaviour of River Welland sand under cyclic loading (Test data after Barden *et al.*[28])

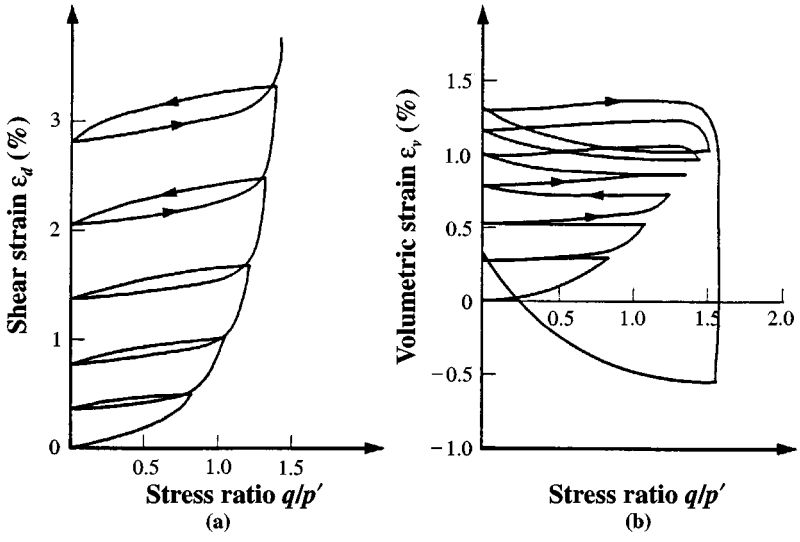

Figure 17. The behaviour of Fuji sand under cyclic loading (after Tatsuoka[18])

of the stress ratio variation. These quantities are defined as

$$\eta_{\mathrm{m}} = 0{\cdot}5\left[\left(\frac{q}{p'}\right)_{\max} + \left(\frac{q}{p'}\right)_{\min}\right] \tag{31}$$

and

$$\eta_{\mathrm{d}} = \left(\frac{q}{p'}\right)_{\max} - \left(\frac{q}{p'}\right)_{\min} \tag{32}$$

5.4.1. Drained cyclic triaxial test. The first set of the tests described here involves application of 50 cycles, and the stress path in (p', q) space follows a straight line between A (100, 0) kPa and B (180, 240) kPa. The soil was initially heavily overconsolidated with $p'_0 = 500$ kPa. The initial voids ratio was 1·02. Predictions of the behaviour under the uniform cyclic loading are shown in Figures 18(a) and 18(b), where the variation of volumetric strain and axial strain with stress ratio and the number of cycles are indicated. Typical data of soil behaviour reported by Linton *et al.*[30] are shown in Figure 19 for the variation of axial strain with deviatoric stress. Experimental data on the variation of volumetric strain during cyclic shearing can also be found in Figure 17(b). The following features of the ideal soil behaviour are predicted.

1. The behaviour in the first cycle differs significantly from that in the following cycles. After four or five cycles, only a very little difference exists between successive cycles. There is a steady transition between the first cycle and the fifth cycle.
2. The rates of development of volumetric and distortional strain during the cyclic loading are not the same. There is a hysteretic loop for the distortional strain. However, there is no such loop for the volumetric strain.

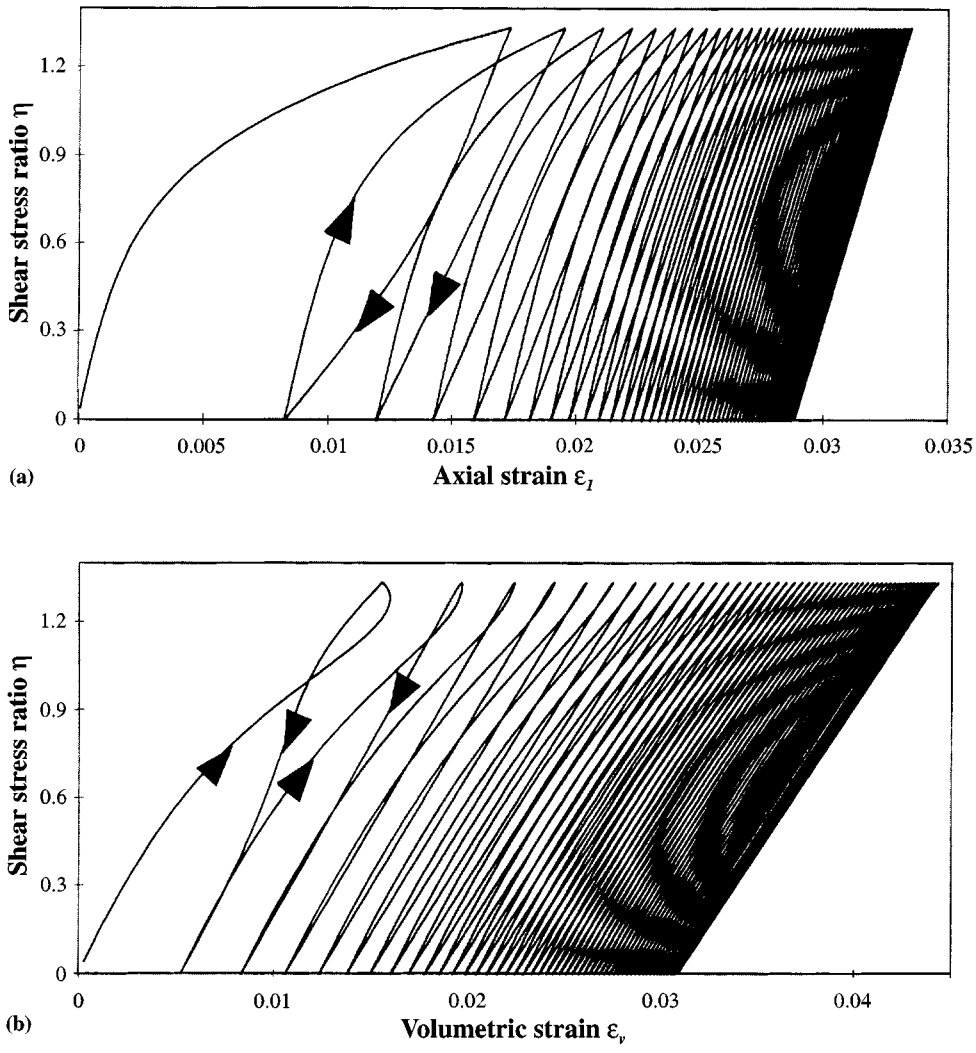

Figure 18. Soil behaviour under cyclic loading ($N = 50$)

3. Permanent volumetric and axial strains are produced in one cycle. The magnitudes of both residual strains decrease with the number of cycles.
4. Volumetric contraction is observed for stress changes with $\eta < M$, and expansion is found for $\eta > M$.
5. Cyclic shearing is effective in densifying the soil. In this case, an accumulation of 3·1 per cent permanent volumetric strain is produced after 50 cycles.

Experimental data on soil behaviour during cyclic loading can be found from research work such as in References 18, 19, 21, 31 and 32, and these data show trends similar to those predicted by this model.

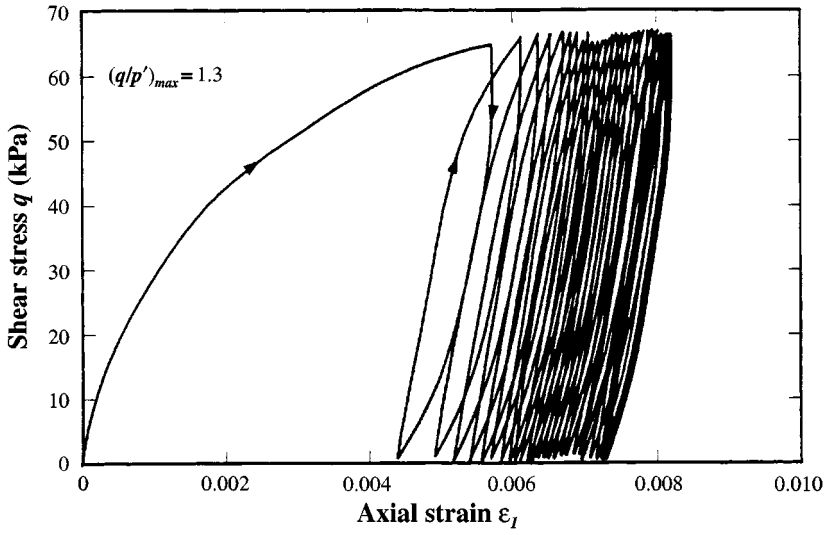

Figure 19. The behaviour of Reid–Bedford sand during cyclic loding ($N = 100$, test data after Linton *et al.*[30])

5.4.2. Effect of average stress ratio and initial density. The second set of calculations involves application of 10,000 cycles under fully drained conditions to three heavily overconsolidated soil specimens. Initially, the specimens were identical with $p'_0 = 1000$ kPa. Each specimen was subjected to a different form of cyclic loading, but the amplitude in each is the same, given by $\eta_d = 0{\cdot}5$. For the first test, $\eta_m = 1{\cdot}25$, in the second $\eta_m = 0{\cdot}75$ and in the third $\eta_m = 0{\cdot}25$. Specifically, in the first test the stress state (p', q) varies cyclically between (150, 150) and (200, 300) kPa; for the second test, between (120, 60) and (150, 150) kPa; and for the third test, between (100, 0) and (120, 60) kPa. The predicted responses are shown in several figures. Figure 20(a) shows the variation of the size of the virgin yield surface with the number of cycles, N, for all three tests. Figure 20(b) shows the relationship between the voids ratio and N, while the variation of volumetric strain with N is indicated in Figures 20(c) and 20(d).

The third set of numerical tests is similar to the second. The differences are as follows:

1. the soil is normally consolidated to the initial stress state, and virgin yielding occurs for the first loading, and
2. the first test in the second set is replaced by a new test with $\eta_m = 0{\cdot}5$, for which the corresponding variation in stress is from (109, 27) to (133·3, 100) kPa.

The predictions for these cases are shown in Figures 21(a)–21(d).

Some experimental data on repeated loading are shown here for qualitative comparison. The experimental data shown in Figure 22 are from simple shear tests carried out by Tokue,[33] and τ/σ'_{yy} is the ratio of shear stress to vertical effective stress. The variation of voids ratio with the number of cycles can be seen from the data. The variation of volumetric strain with the number of cycles is shown in Figure 23 for tests carried out by Kaggwa[32] in a conventional triaxial apparatus on a carbonate sand. The variation of axial strain with the number of cycles is shown in Figure 24,[34] where the material was a very dense sand. El-Sohby[16] performed cyclic loading with constant stress ratio on a dense fine sand under high stress ratio, i.e. $\sigma'_1/\sigma'_3 = 4{\cdot}5$. After two cycles,

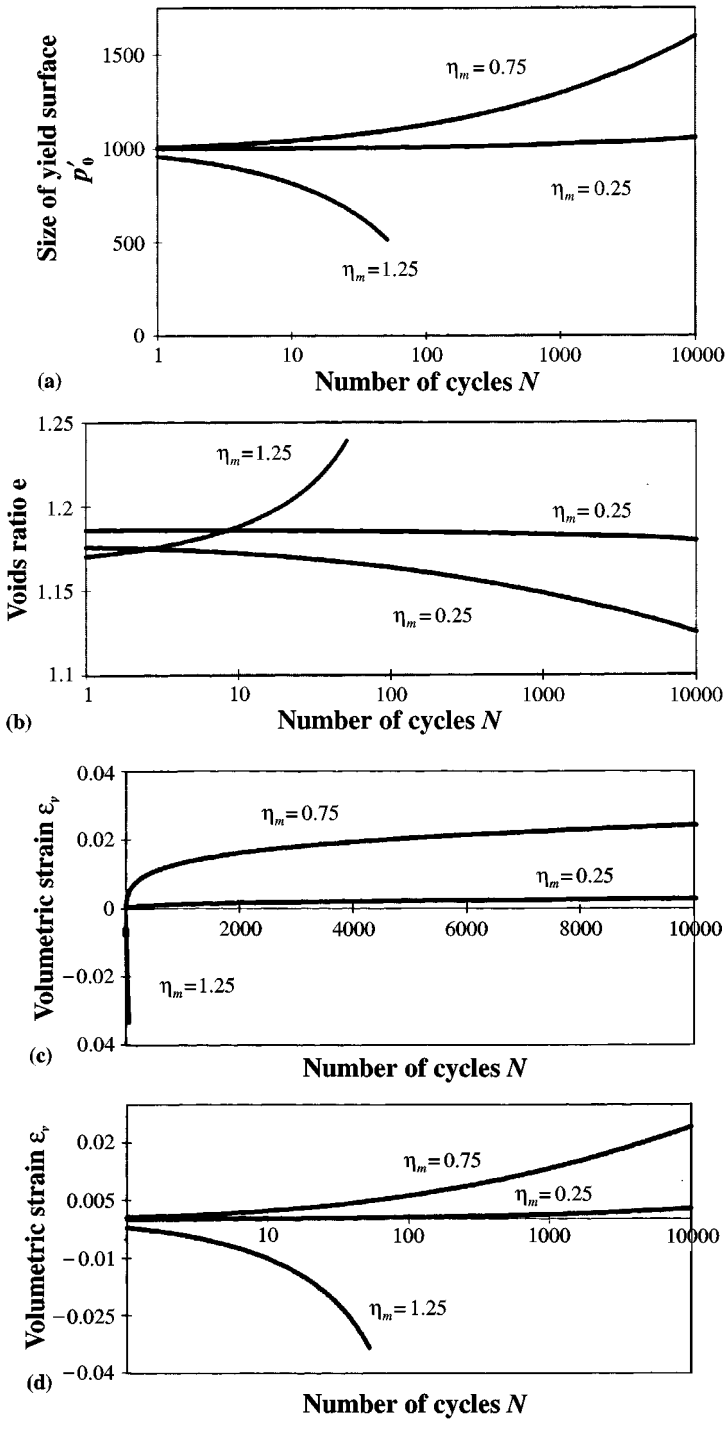

Figure 20. Deformation of dense soil over 10,000 cycles

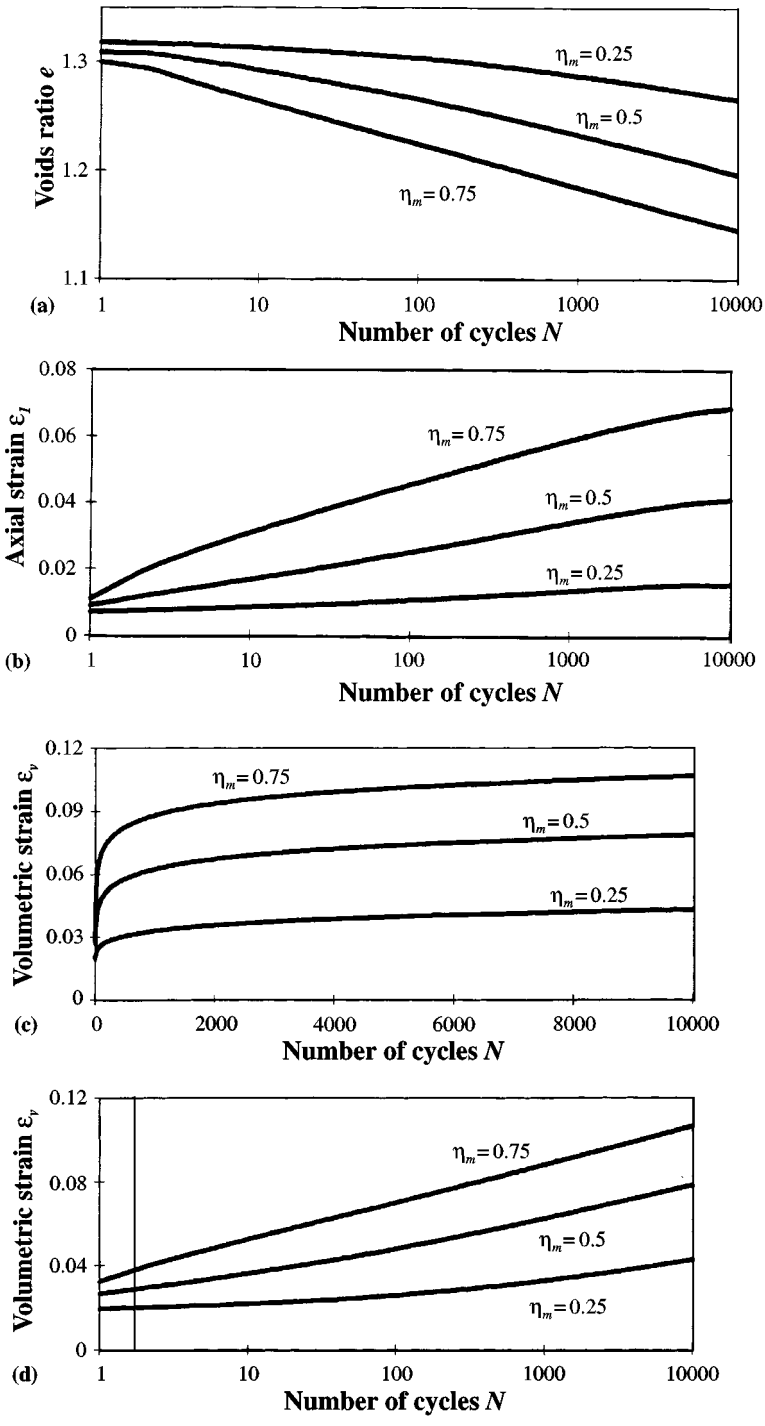

Figure 21. Deformation of loose soil over 10,000 cycles

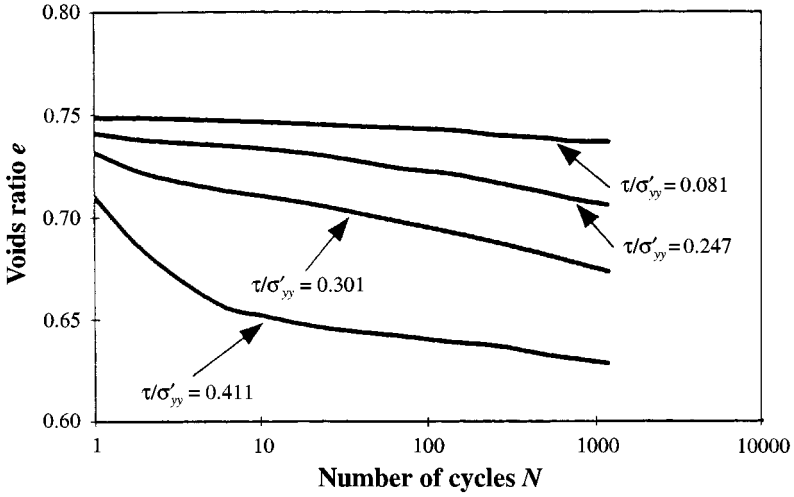

Figure 22. Experimental data on the variation of voids ratio with the number of cycles (Test data after Tokue[33])

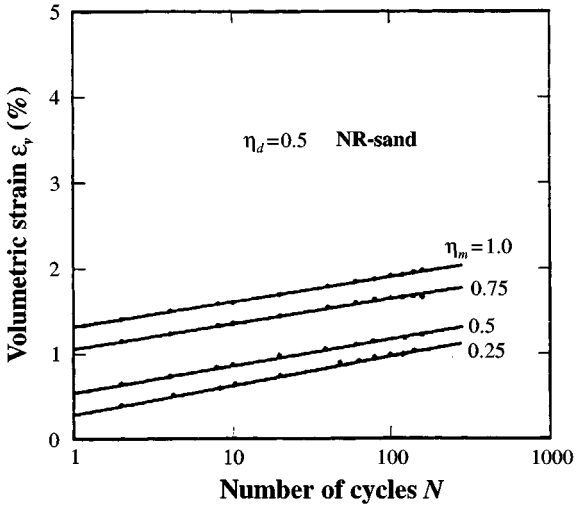

Figure 23. Volumetric deformation of North Rankin sand under cyclic shearing (Test data after Kaggwa[32])

an accumulation of 2·5 per cent permanent volumetric strain was observed, and failure occurred because the sample had been loosened. The trends predicted by this model (Figures 20 and 21) are consistent with these experimental observations.

It is clear from the comparison of the predictions with the experimental data described above that the introduction of Postulate III into a relatively simple constitutive model such as modified Cam Clay has resulted in the following improvements and additional capabilities.

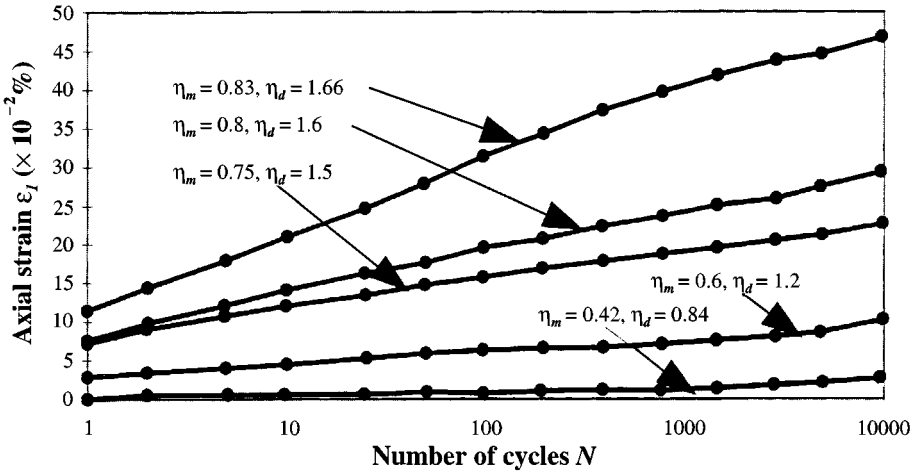

Figure 24. Variation of axial strain with number of cycles on highway subgrade sand (Test data after Lentz *et al.*[34])

For cyclic loading with $\eta < M$:

1. Both permanent volumetric strain (contraction) and axial strain increase monotonically with the number of cycles. Their magnitudes are inversely proportional to soil density.
2. For the cases examined, the permanent residual volumetric strain is approximately linear with the logarithm of N.
3. There is a limit to the permanent volumetric strain that develops as N increases.
4. The size of the virgin yield surface increases with the number of cycles. There is also a limit on p'_0 during cycling.
5. Cyclic shearing causes a decrease in the voids ratio. The contribution from the change in shear stress is generally much greater than that from the change in mean stress. Cyclic shearing is therefore more effective to densify soil. The magnitude of this effect is proportional to the amplitude of the cyclic stress ratio.

For cyclic loading with $\eta > M$:

1. Expansive permanent volumetric strain is produced.
2. Cyclic shearing in this range is unstable. This instability can be seen from the relationships between permanent volumetric strain and number of cycles, and also the relationships between size of the yield surface and number of cycles.
3. Because the soil is overconsolidated at the beginning of the cyclic testing, it can sustain a stress ratio higher than M. During the subsequent cyclic loading, expansive volumetric strain is induced, and the size of the virgin yield surface shrinks. This volumetric expansion and yield surface shrinkage continue under the cyclic loading until, eventually, the current stress ratio becomes higher than the peak strength of the soil and failure occurs.
4. Similar to point (5) in the above paragraph, cyclic shearing with $\eta > M$ is effective in loosening the soil.

The above features predicted are confirmed by experimental data, and details can be found from a general review of the zone for dilation and contraction and instability of soil under cyclic loading by Muir Wood.[31]

6. CONCLUSION

The fundamental concept underlying the soil models described in this paper is that the material exhibits plastic volumetric deformation hardening. Three types of material idealization have been proposed to describe this behaviour. They are an elastic and virgin-yielding material, a sub-yielding and virgin-yielding material, and a material that allows elastic, sub-yielding and virgin-yielding behaviour. The corresponding incremental forms of the hardening formulae have also been presented. Any of the three postulates can be implemented easily into most constitutive models that include volumetric-strain-controlled hardening.

As a particular illustration, all postulates have been implemented into the well-known modified Cam Clay model. The predictions of the new models developed have been demonstrated in detail. It was found that Postulate I provides a simple and acceptable modelling for problems where only virigin yielding occurs and the details of soil behaviour during reloading are not important. Postulate II provides a satisfactory description for problems where there is a need to determine accurately soil deformation under subsequent loading for a small number of cycles. Postulate III provides a good practical model for soil behaviour where interest lies in predicting the behaviour under a large number of cycles of repeated loading.

ACKNOWLEDGEMENTS

The work described in this paper forms part of an overall research programme investigating the constitutive behaviour of fissured and structured soils. This work is supported by a grant from the Australian Research Council.

REFERENCES

1. A. N. Schofield and C. P. Wroth, *Crticial State Soil Mechanics*, MacGraw-Hill, London, 1968.
2. J. P. Carter, J. R. Booker and C. P. Wroth, 'A critical state model for cyclic loading', in Pande *et al.* (eds), *Soil Mechanics – Transient & Cyclic Loading*, 1982, pp. 219–252.
3. Z. Mroz, V. A. Norris and O. C. Zienkiewicz, 'An anisotropic, critical state model for soils subject to cyclic loding', *Géotechnique*, **31**(4)**,** 451–469 (1981).
4. K. Hashiguchi, 'Macrometric approaches – static – intrinsically time-independent', *Proc. 11th Int. Conf. Soil Mechanics & Foundation Engineering*, 1985, pp. 25–56.
5. C. S. Desai and J. Toth, 'Disturbed state constitutive modelling based on stress-strain and non-destructive behaviour', *Int. J. Solids Struct*, **33**(11)**,** 1619–1650 (1996).
6. A. Baltov and A. Sawczuk, 'A rule for anisotropic hardening', *Acta Mech.*, **I/2,** pp. 81–92 (1965).
7. M. D. Liu, 'A constitutive model for sand and its application', *Ph.D. Thesis*, Glasgow University, 1991.
8. W. D. Iwan, 'On a class of models for the yielding behaviour of continuous and composite systems', *J. Appl. Mech., Trans. ASCE*, **34,** 612–617 (1967).
9. Z. Mroz, 'An attempt to describe the behaviour of metal under cyclic loads using a more general workhardening model', *Acta Mech.*, **2,** 199–212 (1969).
10. R. F. Scott, 'Plasticitiy and constitutive relations in soil mechanics', *J. Geotech. Engng.*, ASCE, **111**(5)**,** 563–605 (1985).
11. Y. Meimon and C. Tan, 'A new double hardening model for soils under cyclic loding', in Pietruszczak *et al.* (eds), *Numerical Models in Geomechanics NUMOG III*, 1989 pp. 28–35.
12. K. Hashiguchi, 'Constitutive equations of elastoplastic materials with anisotropic hardening and elastic-plastic translation', *J. Appl. Mech.*, ASME, **48,** 297–301 (1981).
13. A. Gens and D. M. Potts, 'Critical state models in computational geomechanics', *Engng. Comput.*, **5,** 178–197 (1998).
14. M. S. Rahman, H. B. Seed and J. R. Booker, 'Pore pressure development under offshore gravity structures', *J. Geotech. Engng.*, ASCE, **103**(12)**,** 1419–1436 (1977).
15. W. D. L. Finn, 'Dynamic response analyses of saturated sands', in Pande *et al.* (eds). *Soil Mechanics-transient & Cyclic Loading*, 1982, pp. 105–132.
16. M. A. El-Sohby, 'The behaviour of particulate materials under stress', *Ph.D. Thesis*, Manchester University, 1964.

17. R. W. Sarsby, 'The deformation behaviour of particulate media subjected to constant stress paths', *M.Sc. Thesis*, Manchester University, 1978.
18. F. Tatsuoka, 'Shear tests in a triaxial apparatus – a fundamental study of the deformation of sand', *Ph.D. Thesis*, Tokyo University, 1972.
19. Y. Yamada, 'Deformation characteristics of loose sand under three dimensional stress conditions', *Ph.D. Thesis*, Tokyo University, 1979.
20. M. P. Luong, 'Stress-strain aspects of cohesionless soil under cyclic and transient loads', in Pande *et al.* (eds). *Soil under Cyclic & Transient Loading*, 1980, pp. 315–324.
21. D. W. Airey, 'Clays in circular simple shear apparatus', *Ph.D. Thesis*, Cambridge University (1984).
22. T. S. B. Pradhan, F. Tatsuoka and Y. Sata, 'Experimental stress-dilatancy relations of sand subjected to cyclic loading', *Soils and Found.*, **29**(1)**,** 45–67 (1989).
23. G. Castro, 'On the behaviour of soils during earthquakes-liquefaction', in Cakmar (ed), *Soil Dynamics and Liquefaction*, Computational Mechanics Publications (1987).
24. D. Muir-Wood, *Soil Behaviour and Critical State Soil Mechanics*, Cambridge University Press, Cambridge, 1990.
25. R. Butterfield and F. Baligh, 'A new evaluation of loading cycles in an oedometer', *Géotechnique*, **46**(3)**,** 547–553 (1996).
26. K. Been and M. G. Jefferies, 'A state parameter for sands', *Géotechnique*, **35**(1)**,** 99–112 (1985).
27. M. Bolton, 'The strength and dilatancy of sands', *Géotechnique*, **36**(1)**,** 65–78 (1986).
28. L. Barden, A. J. Khayatt and A. Wightman, 'Elastic and slip components of the deformation of sand', *Canad. Geotech. J.* **6**(3)**,** 227–239 (1969).
29. Y. Sheng, 'A constitutive model for monotonic and cyclic behaviour of sands', *Ph.D. Thesis*, University of Western Australia, 1995.
30. P. F. Linton, M. C. McVay and D. Bloomquist, 'Measurement of deformations in the standard triaxial environment with a comparison of local versus global measurements on a fine, fully drained sand', in Donaghe *et al.* (eds), *Advanced Triaxial Testing of Soils and Rock*, 1988, pp. 202–215.
31. D. Muir-Wood, 'Laboratory investigations of the behaviour of soils under cyclic loading: a review', in Pande *et al.* (eds) *Soil Mechanics – Transient & Cyclic Loading*, 1982, pp. 513–582.
32. W. S. Kaggwa, 'Cyclic behaviour of carbonate sediments, *Ph.D. Thesis*, Sydney University, 1988.
33. T. Tokue, 'Deformation behaviours of dry sand under cyclic loading and stress-dilatancy model', *Soild Found.*, **19**(2)**,** 65–76 (1979).
34. R. W. Lentz and G. Y. Baladi, 'Simplififed procedure to characterise permanent strain in sand subjected to cyclic loading', in Pande *et al.* (eds), *Soil Under Cyclic & Transient Loading*, Wiley, 1980, pp. 89–95.

